Rajadurai et al., http://www.jcb.org/cgi/content/full/jcb.201501003/DC1

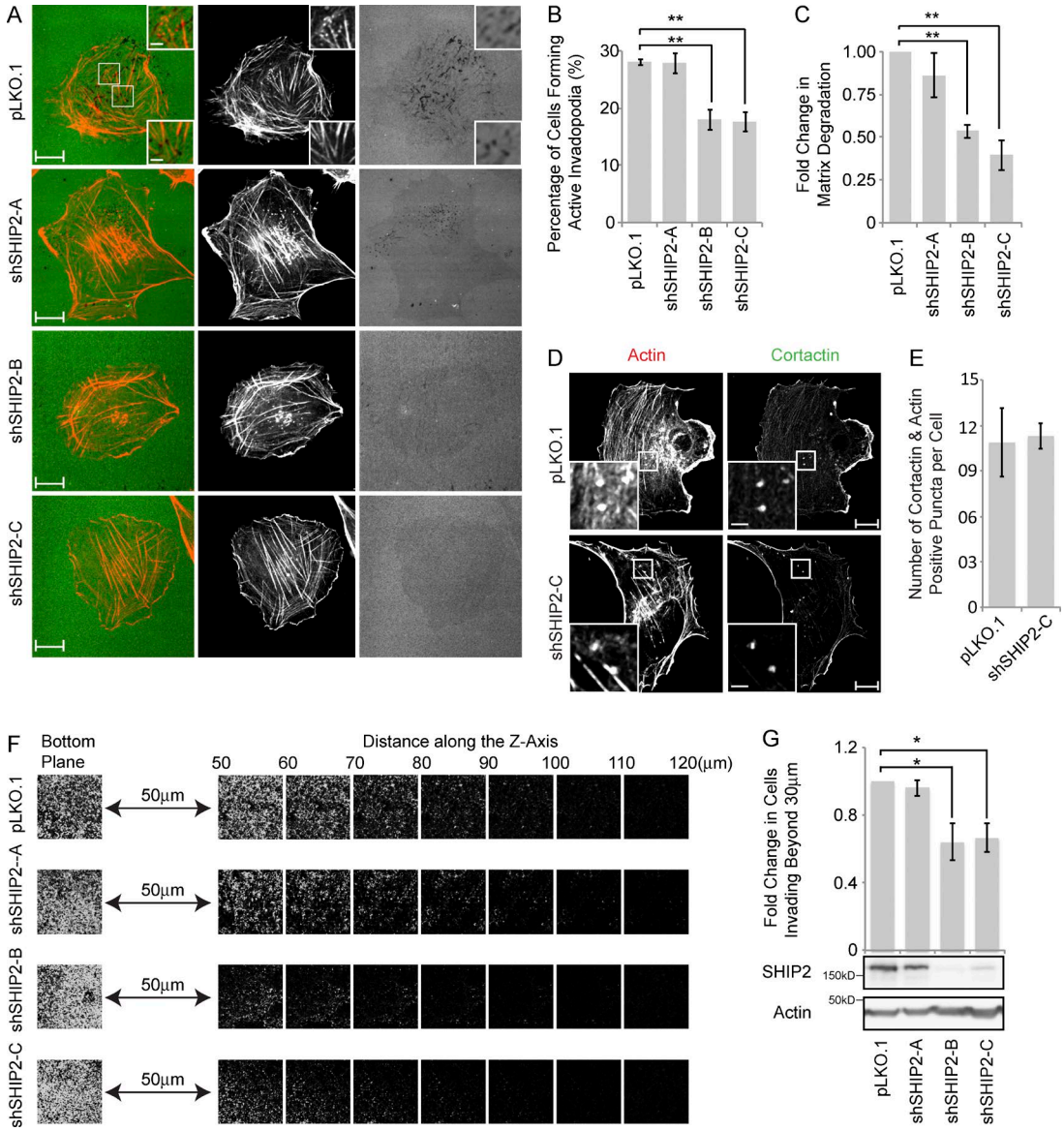

Figure S1. **SHIP2 is required for maturation of invadopodia competent for ECM degradation and cancer cell invasion.** (A) MDA-MB-231 cells stably transduced with lentiviral vector pLKO.1, pLKO.1 carrying noneffective shRNA duplex, or two shRNA duplexes targeting SHIP2 were seeded on fluorescently labeled gelatin and stained with phalloidin (F-actin), and confocal images were acquired. (B) Percentage of SHIP2 knockdown cells that form proteolytically active invadopodia (positive for F-actin punctate overlaying matrix degradation area) was quantified in comparison to control cells. (C) Amount of ECM degradation (mean matrix degradation area per fields of view) by SHIP2-knockdown cells was quantified as fold change compared with control cells. (D) SHIP2-knockdown MDA-MB-231 and control cells were seeded on unconjugated-gelatin matrices and immunostained for invadopodia markers, F-actin and cortactin, and confocal images of the ventral cell surfaces were acquired. (E) F-actin–positive and cortactin-positive punctae in SHIP2-knockdown MDA-MB-231 and control cells were quantified from 30 images acquired in three independent experiments. (F) MDA-MB-231 cells stably transduced with pLKO.1 lentiviral vector alone or pLKO.1 lentiviral vectors containing two individual shRNA duplexes targeting SHIP2, as well as one nonsilencing shRNA, were subjected to an inverted invasion assay. Representative confocal *z*-stack from each condition depicts relative cell invasion. (G) For quantification of cell invasion, five confocal *z*-stacks per condition per experiment were acquired. Fluorescence intensity of the planes within each *z*-stack was measured using Cell Profiler software. Cells invading to and past 30 µm inside the matrix were quantified as percentage of total cell population. Experiments were repeated four times. Western blot shows the relative protein levels of SHIP2 between different MDA-MB-231 cells stably transduced with pLKO.1, SHIP2-targeting shRNA duplexes, and noneffective shRNA. All quantified data indicate the mean values ± SE from at least four independent experiments. *, $P < 0.05$; **, $P < 0.01$. Bars: 10 µm; (inset) 2 µm.

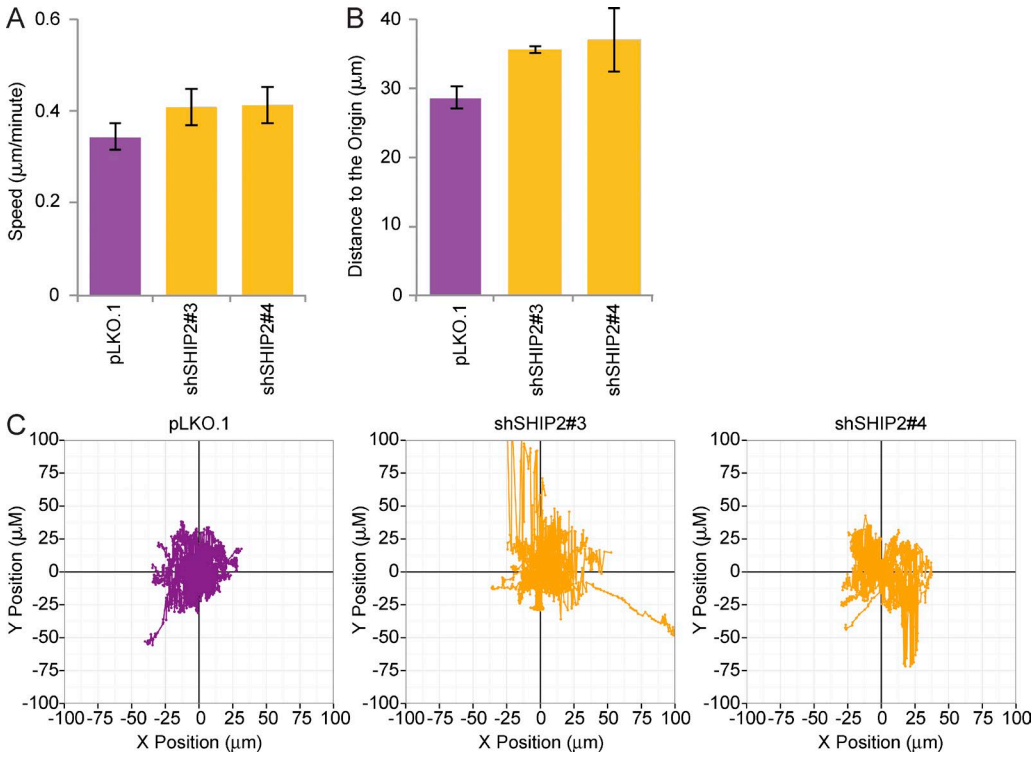

Figure S2. **SHIP2 depletion does not affect random cell migration.** (A) MDA-MB-231 cells stably transduced with lentiviral vector pLKO.1, pLKO.1 carrying two shRNA duplexes targeting SHIP2 were seeded on six-well dishes and subjected to time-lapse video microscopy (phase contrast). Images were acquired every 5 min for 24 h. The last 8 h of this video was analyzed, and cell migration speed of 75 cells was measured based on 15 videos from three independent experiments. (B) As in A, time-lapse imaging was performed, and distance to the origin of 75 cells was measured based on 15 videos from three independent experiments. (C) As in A, time-lapse imaging was performed; track plot depicts migration pattern of 25 MDA-MB-231-pLKO.1, MDA-MB-231-shSHIP2#3, and MDA-MB-231 shSHIP2#4 cells based on five videos from one independent experiment. All quantified data indicate the mean values ± SE from at least three independent experiments.

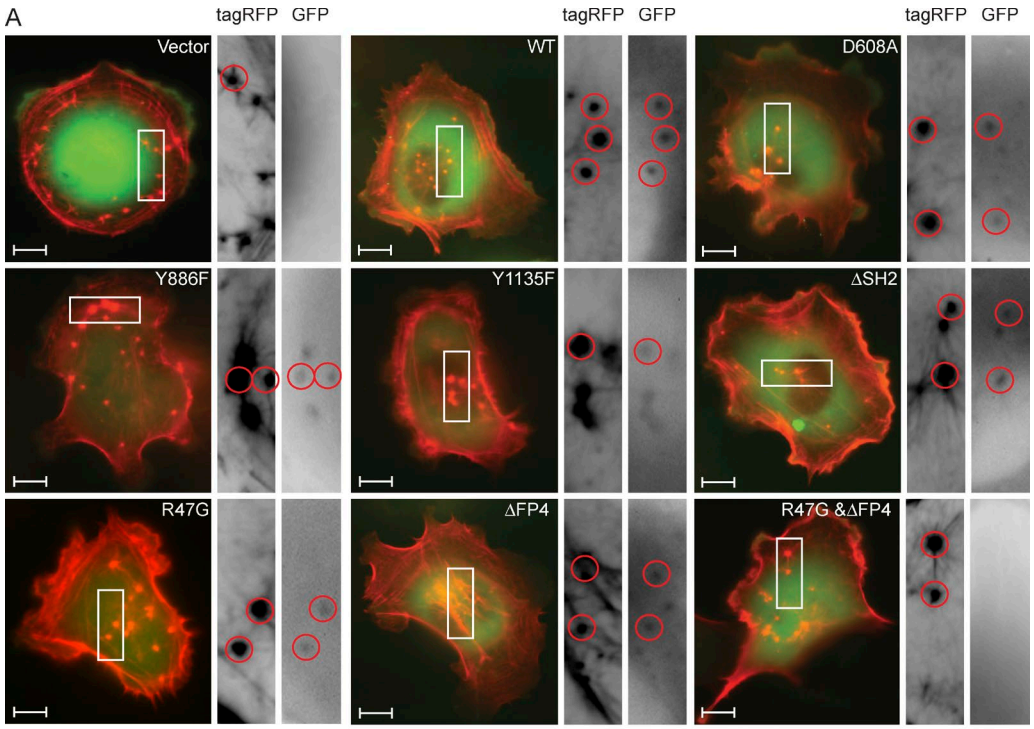

B

Construct	Localization to Invadopodia
SHIP2	Yes
SHIP2-D608A	Yes
SHIP2-Y886F	Yes
SHIP2-Y1135F	Yes
SHIP2ΔSAM	Yes
SHIP2ΔSH2	Yes
SHIP2-R47G	Yes
SHIP2ΔFP4	Yes
SHIP2-R47G & ΔFP4	No

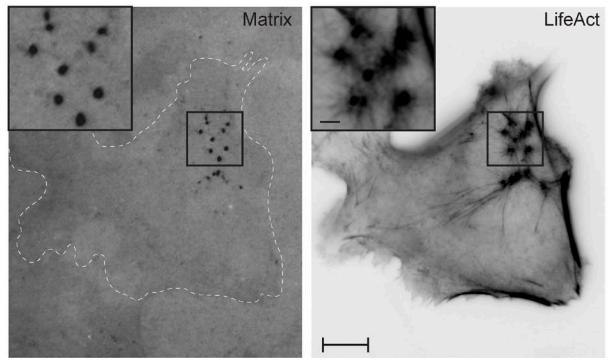

Figure S3. **SHIP2DFP4 and R47G fail to localize to invadopodia.** (A) MDA-MB-231 cells were transiently cotransfected with tagRFP-LifeAct and pEGFP-N3 vector alone, pEGFP-N3-SHIP2- or pEGFP-N3-fused mutants of SHIP2 uncoupled from specific binding partners, and catalytically inactive SHIP2 mutant and subjected to time-lapse video microscopy. Single frames from the videos highlight the localization of SHIP2 or SHIP2 mutants with respect to filamentous actin within the invadopodia-like structures. (B) Table summarizes the ability of wild-type SHIP2 and SHIP2 mutants lacking specific domains, mutated to render catalytically inactive or specific tyrosine residues mutated to phenylalanine to localize to invadopodia. (C) MDA-MB-231 cells were transiently transfected with tagRFP-LifeAct, seeded on fluorescently labeled gelatin, and subjected to time-lapse video microscopy. Single frame from the videos highlight F-actin punctate localization with respect to the areas of the degraded ECM. Bars: 10 µm; (inset) 2 µm.

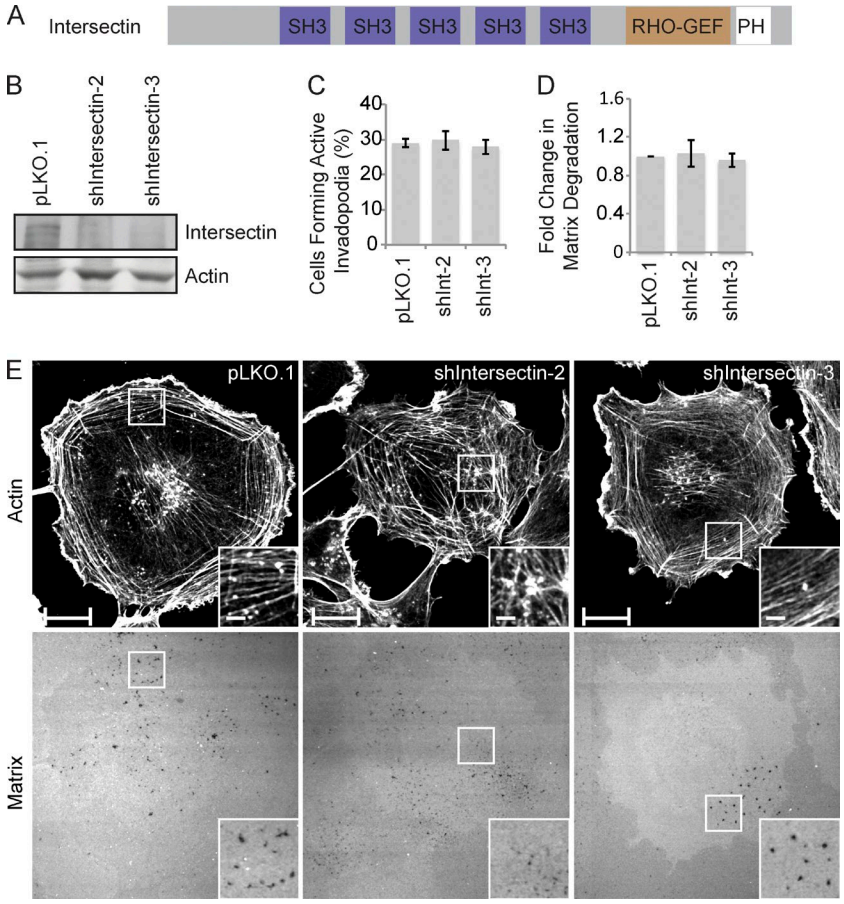

Figure S4. **Intersectin is not required for invadopodia-mediated ECM degradation.** (A) Schematic diagram of Intersectin depicts the domain structure and organization: five SH3 domains, followed by a Rho-GEF domain and a C-terminal PH domain. (B) MDA-MB-231 cells were stably transduced with the lentiviral vector pLKO.1 or two Intersectin shRNA duplexes, and efficiency of shRNA-mediated Intersectin knockdown was assessed by Western blot analysis. (C–E) MDA-MB-231-pLKO.1 and MDA-MB-231-shIntersectin (shIntersectin-2 and shIntersectin-3) cells were seeded on fluorescently labeled gelatin and stained with phalloidin (F-actin), and confocal images were acquired at the ventral surface (E). Bars: 10 µm; (inset) 2 µm. (C) Percentage of Intersectin-knockdown cells that form proteolytically active invadopodia was quantified in comparison to control. (D) Amount of ECM degradation by Intersectin-knockdown cells was quantified as fold change of control. All quantified data indicate the mean values ± SEM from at least three independent experiments.

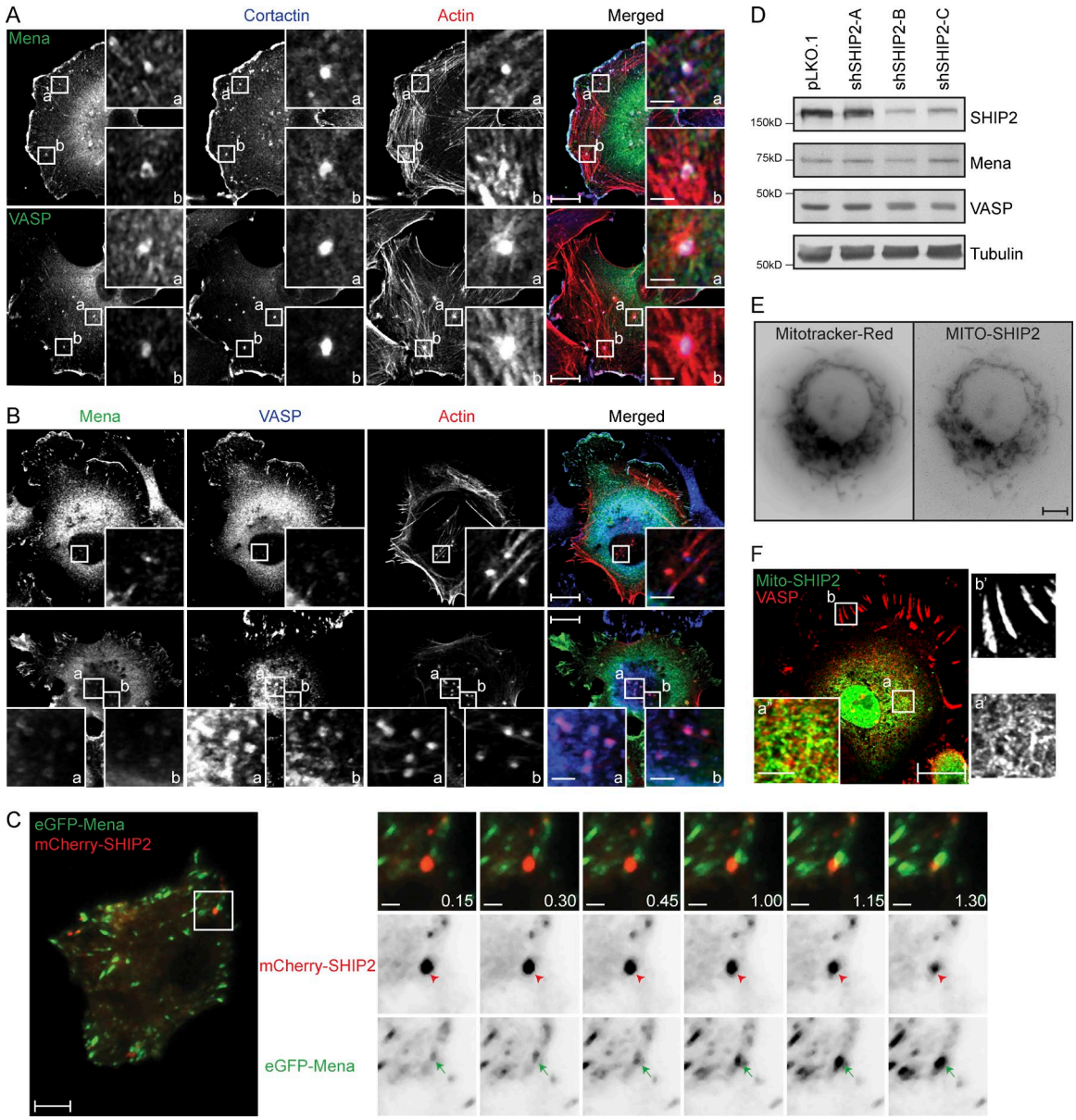

Figure S5. **SHIP2 recruits Mena to subcellular structures.** (A) MDA-MB-231 cells were seeded on unconjugated gelatin matrix and immunostained for Mena or VASP and invadopodia markers F-actin (phalloidin) and cortactin, and confocal images were acquired at the ventral surface. (B) MDA-MB-231 cells were seeded on unconjugated gelatin matrix and immunostained for Mena, VASP, and F-actin (phalloidin), and confocal images were acquired at the ventral surface. (C) mCherry-SHIP2 and GFP-Mena were transiently coexpressed in MDA-MB-231 cells and imaged by the total internal reflection fluorescent microscopy. Montages of the GFP and RFP channels depict the relative localization of Mena and SHIP2. Arrows indicate GFP-Mena localization, and arrowheads indicate mCherry-SHIP2 localization. (D) Under SHIP2-depleted conditions, protein levels of Mena and VASP are examined by Western blot analysis. (E) GFP-tagged mitochondria-targeted SHIP2 (Mito-SHIP2) was transiently expressed in SKBr3 cells and stained with MitoTracker red to establish the localization the Mito-SHIP2 construct. (F) Mito-SHIP2 was transiently expressed in SKBr3 cells and stained for GFP (MITO-SHIP2), and VASP and confocal images were acquired to establish the localization of VASP with respect to Mito-SHIP2. (a′) Localization of Mito-SHIP2 to mitochondria. (b′) Localization of VASP to focal adhesion. (a″) Lack of colocalization between Mito-SHIP2 and VASP. Bars: 10 μm; (insets) 2 μm.

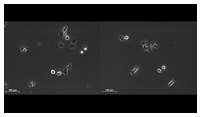

Video 1. **SHIP2 depletion does not affect random cell migration.** MDA-MB-231 cells stably transduced with lentiviral vector pLKO.1 or pLKO.1 carrying shRNA duplex targeting SHIP2 were subjected to phase-contrast video microscopy. Images were acquired every 5 min for 24 h, and the last 8 h of the video is displayed at 3/10 of a second per frame. MDA-MB-231-pLKO.1 cells are displayed on the left and MDA-MB-231-shRNA cells on the right.

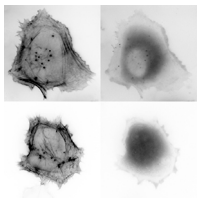

Video 2. **SHIP2ΔFP4-R47G fails to localize to actin-rich invadopodia protrusions.** MDA-MB-231 cells were transiently transfected with tagRFP-LifeAct and either WT-SHIP2 (left) or SHIP2ΔFP4-R47G (right), cultured on unconjugated gelatin matrix for 24 h, and subjected to time-lapse video microscopy. Images were acquired every 15 s for 5 min and are displayed at 3/10 of a second per frame. Bars, 10 µm.

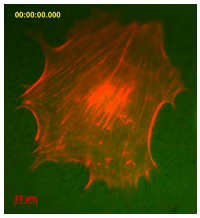

Video 3. **Matrix degradation under actin-rich membrane protrusions.** MDA-MB-231 cells were transiently transfected with tagRFP-LifeAct, cultured on fluorescent matrix for 24 h, and subjected to time-lapse video microscopy. Images were acquired every 15 s for 5 min and are displayed at 3/10 of a second per frame. Bars, 10 µm.

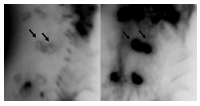

Video 4. **Mena forms a ring around the actin core.** MDA-MB-231 cells were transiently cotransfected with tagRFP-LifeAct and GFP-Mena, cultured on unconjugated matrix for 24 h, and subjected to time-lapse video microscopy. Images were acquired every 15 s for 5 min and are displayed at 3/10 of a second per frame. GFP-Mena is depicted on the left and tagRFP-LifeAct on the right. Bars, 10 µm.

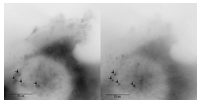

Video 5. **Mena forms a ring around the Tks5 core.** MDA-MB-231 cells were transiently cotransfected with mCherry-Tks5 and GFP-Mena, cultured on unconjugated matrix for 24 h, and subjected to time-lapse video microscopy. Images were acquired every 15 s for 5 min and are displayed at 3/10 of a second per frame. GFP-Mena is depicted on the left and mCherry-Tks5 on the right. Bars, 10 µm.

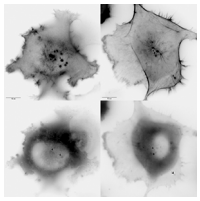

Video 6. **SHIP2 depletion affects Mena localization with respect to actin core.** MDA-MB-231-pLKO.1 or MDA-MB-231-shSHP2 cells were transiently cotransfected with GFP-Mena and tagRFP-LifeAct, cultured on gelatin matrix for 24 h, and subjected to time-lapse video microscopy. Images were acquired every 15 s for 5 min and are displayed at 3/10 of a second per frame. MDA-MB-231-pLKO.1 is depicted on the left and MDA-MB-231-shSHP2 on the right. Bars, 10 µm.

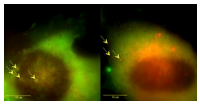

Video 7. **SHIP2 depletion affects Mena localization with respect to Tks5 core.** MDA-MB-231-pLKO.1 or MDA-MB-231-shSHP2 cells were transiently cotransfected with GFP-Mena and mCherry-Mena, cultured on gelatin matrix for 24 h, and subjected to time-lapse video microscopy. Images were acquired every 15 s for 5 min and are displayed at 3/10 of a second per frame. MDA-MB-231-pLKO.1 is depicted on the left and MDA-MB-231-shSHP2 on the right. Bars, 10 µm.

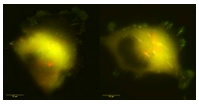

Video 8. **SHIP2 depletion does not affect Mena localization to Paxillin-positive focal adhesions.** MDA-MB-231 cells were transiently cotransfected with mCherry-Paxillin and GFP-Mena, cultured on gelatin matrix for 24 h, and subjected to time-lapse video microscopy. Images were acquired every 15 s for 5 min and are displayed at 3/10 of a second per frame. MDA-MB-231-pLKO.1 is depicted on the left and MDA-MB-231-shSHIP2 on the right. Bars, 10 μm.

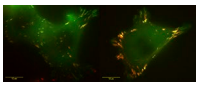

Video 9. **SHIP2 depletion does not affect Mena localization to Zyxin-positive focal adhesions.** MDA-MB-231 cells were transiently cotransfected with mCherry-Zyxin and GFP-Mena, cultured on gelatin matrix for 24 h, and subjected to time-lapse video microscopy. Images were acquired every 15 s for 5 min and are displayed at 3/10 of a second per frame. MDA-MB-231-pLKO.1 is depicted on the left and MDA-MB-231-shSHIP2 on the right. Bars, 10 μm.

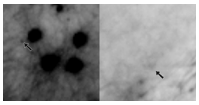

Video 10. **SHIP2 uncoupled from Mena destabilizes actin-rich membrane protrusions.** SHIP2-depleted MDA-MB-231 cells were rescued with either WT-SHIP2 or SHIP2ΔFP4, transiently transfected with tagRFP-LifeAct, cultured on unconjugated matrix for 24 h, and subjected to time-lapse video microscopy. Images were acquired every 5 s for 5 min and are displayed at 3/10 of a second per frame. Actin-rich membrane protrusions found in SHIP2-knockdown cells rescued with WT-SHIP2 are depicted on the left and F-actin protrusions from SHIP2 knockdown cells rescued with SHIP2ΔFP4 on the right.